International Symposium
On Turbulence and Shear Flow
Phenomena (TSFP-8)
August 28 - 30, 2013 Poitiers, France

SLIP VELOCITY OF RIGID FIBERS IN A TURBULENT CHANNEL FLOW

Lihao Zhao
Department of Energy and Process Engineering
Norwegian University of Science and Technology
Trondheim, Norway
lihao.zhao@ntnu.no

Cristian Marchioli
Department of Energy Technology
University of Udine
Udine, Italy
cristian.marchioli@uniud.it

Helge I. Andersson
Department of Energy and Process Engineering
Norwegian University of Science and Technology
Trondheim, Norway
helge.i.andersson@ntnu.no

ABSTRACT

In the current study the slip velocity between rigid fibers and a viscous fluid is investigated in a turbulent channel flow. The statistical moments of the slip velocity are evaluated considering prolate ellipsoidal fibers with Stokes number, St, ranging from 1 to 100 and aspect ratio, λ, ranging from 3 to 50. Statistics are compared one-to-one with those obtained for spherical particles ($\lambda = 1$) to highlight effects due to fiber elongation. The statistical results show that the effect of Stokes number is found to be important and there is a monotonic dependence that the magnitude of slip velocity becomes larger with increasing Stokes number. However, the influence of aspect ratio is relatively weaker than the Stokes number effect. And the non-monotonic aspect ratio dependence is observed in both streamwise and wall-normal slip velocity. The smallest fiber deposition is found at aspect ratio $\lambda = 50$ with minimum value of slip velocity in wall-normal direction.

Introduction

Particle dynamics in turbulent wall flows have been investigated from a variety of different points of view. Particulate flow can be found in industrial applications such as in chemical processing and pneumatic transport, and in nature, like sand storms and in rivers. A vast number of studies on suspensions of spherical particles have been performed during the years. However, non-spherical particles are also commonly occurring, for instance in paper making, but suspensions of anisotropic particles have received only modest attention. The behaviour of elongated (i.e. non-spherical) particles has recently been studied by Manhart (2003), Paschkewitz et al. (2004), Gillissen et al. (2008) and Andersson et al. (2012) with different representation of the particles. The present work is aimed to explore the slip velocity of elongated rigid fibers in a turbulent channel flow. We follow an approach in which both the fluid flow and the particle motion are based on so-called 'first principles', i.e. the fundamental laws of mechanics. The flow field is obtained directly from the Navier-Stokes equations by means of direct numerical simulations (DNS) while the particle dynamics is governed by equations of translational and rotational motion for each and every individual particle. This is known as the Euler-Lagrangian approach and has already been used to study motions of elongated fiber-like particles in laminar flows by for instance Lundell & Carlsson (2010) and in turbulent flows by Zhang et al. (2001), Mortensen et al. (2008) and Marchioli et al. (2010).

MATHEMATICAL MODELING

The turbulent flow of a dilute suspension of rigid fibers in a plane channel is represented by a Lagrangian-Eulerian approach. In this section the Eulerian formulation of the fluid phase is provided first and followed by the Lagrangian representation of the rigid fibers.

Eulerian fluid representation

In present work the carrier fluid is Newtonian and isothermal and the motion is governed by the mass continuity and momentum equations for an incompressible fluid:

$$\nabla \cdot \mathbf{u} = 0; \qquad \frac{\partial \mathbf{u}}{\partial t} + (\mathbf{u} \cdot \nabla)\mathbf{u} = -\nabla p + \frac{1}{Re_\tau}\nabla^2 \mathbf{u} \qquad (1)$$

where $\mathbf{u} = u\mathbf{i} + v\mathbf{j} + w\mathbf{k}$ and p denote the fluid velocity vector and the pressure, respectively. Here $\mathbf{i}$, $\mathbf{j}$ and $\mathbf{k}$ are the unit vectors in a Cartesian coordinate system. The frictional Reynolds number $Re_\tau = hu_\tau/\nu$ is based on the height h of the channel, the kinematic viscosity ν of the fluid, and the wall-friction velocity u_τ, where u_τ is defined in terms of the wall shear stress τ_{wall} as $(\tau_{wall}/\rho)^{1/2}$.

The flow is driven through the plane channel by a constant mean pressure gradient in the positive x-direction. The turbulent channel flow is totally unaffected by the presence of the fibers, i.e. there is no reaction force from the fibers in the fluid momentum equation (1). The present study is

therefore one-way coupled and this simplification is justified for sufficient dilute fiber suspensions.

Lagrangian representation of rigid fiber

Rigid fibers are elongated non-spherical particles which can be modeled as prolate spheroids, i.e. biaxial ellipsoids with the major axis exceeding the two identical minor axes.

The motion of spheroidal particles in a Newtonian fluid with mass m and aspect ratio $\lambda = b/a$ where a and b are the semi-minor and semi-major axes, respectively. The mathematical modeling of the spheroidal point-particles follows the methodology outlined by Zhang et al. (2001) and subsequently adopted by Mortensen et al. (2008) and Marchioli et al. (2010). The translational and rotational motion of one single fiber is governed by:

$$m\frac{d\mathbf{u}_p}{dt} = \mathbf{F}, \qquad \frac{d(\mathbf{I}\cdot\boldsymbol{\omega}')}{dt} + \boldsymbol{\omega}' \times (\mathbf{I}\cdot\boldsymbol{\omega}') = \mathbf{N}'. \tag{2}$$

Two different Cartesian frames of reference are used. Newton's 2^{nd} law of motion (2a) is expressed in an *inertial frame* $x_i =< x,y,z >$ and Euler's equation (2b) is formulated in the *frame* $x_i' =< x',y',z' >$ with its origin at the fiber mass center and the coordinate axes aligned with the principal directions of inertia. Thus, $\mathbf{u}_p = d\mathbf{x}/dt$ denotes the translational fiber velocity in the inertial frame whereas $\boldsymbol{\omega}'$ is the angular velocity of the fiber in the particle frame and $\mathbf{I}$ is the moment of inertia tensor for the fibers.

If the fibers are sufficiently small so that the neighboring flow can be considered as Stokesian, the force $\mathbf{F}$ acting on a fiber from the surrounding fluid can be expressed as:

$$\mathbf{F} = \mu\mathbf{A}^t\mathbf{K}'\mathbf{A}(\mathbf{u}_f - \mathbf{u}_p) \tag{3}$$

where $\mathbf{u}_f$ is the fluid velocity at the fiber position Here, $\mathbf{A}$ denotes the orthogonal transformation matrix which relates the same vector in the two different frames through the linear transformation $x_i = A_{ij}x_j'$. The expression for the hydrodynamic drag force on a non-spherical particle was derived by Brenner (1964). According to eq. (2), which is valid only when the fiber Reynolds number $Re_p =\mid \mathbf{u}_f - \mathbf{u}_p \mid a/\nu$ is low, the force acting on the fiber is therefore linearly dependent on the difference in translational velocity between the local fluid and the fiber, i.e. the slip velocity $\Delta\mathbf{u} = \mathbf{u}_f - \mathbf{u}_p$. The local fluid vector can be decomposed as u_f, v_f and w_f into three directions x, y and z, respectively. Similarly for the fiber velocity u_p, v_p, w_p are particle velocity components which consists the fiber velocity $\mathbf{u}_p$.

Similarly, the torque N_i' is dependent on the difference in angular velocity between the fluid and the particle, i.e. $\Delta\boldsymbol{\omega}'=\boldsymbol{\Omega}' - \boldsymbol{\omega}'$:

$$\begin{aligned} N_1' &= \tfrac{16\pi\mu a^3\lambda}{3(\beta_0+\lambda^2\gamma_0)}[(1-\lambda^2)S_{23}' + (1+\lambda^2)(\Omega_1' - \omega_1')] \\ N_2' &= \tfrac{16\pi\mu a^3\lambda}{3(\alpha_0+\lambda^2\gamma_0)}[(\lambda^2-1)S_{13}' + (1+\lambda^2)(\Omega_2' - \omega_2')] \\ N_3' &= \tfrac{32\pi\mu a^3\lambda}{3(\alpha_0+\beta_0)}(\Omega_3' - \omega_3'). \end{aligned} \tag{4}$$

Here, S_{ij}' and Ω_i' denote the fluid rate-of-strain tensor and rate-of-rotation vector, respectively. The vorticity of the fluid flow field is thus $2\Omega_i'$. The parameters α_0, β_0 and γ_0 depend on the fiber aspect ratio λ.These expressions were first derived by Jeffery (1922) for an ellipsoidal particle in creeping motion, i.e. $Re_p < 1$.

The shape of a prolate spheroid is characterized by the aspect ratio λ, whereas the ability of the spheroid to adjust to the ambient flow field can be estimated in terms of the response time:

$$\tau = \frac{2\lambda\rho_p a^2}{9\mu}\frac{ln(\lambda+\sqrt{\lambda^2-1})}{\sqrt{\lambda^2-1}}; \qquad St = \frac{\tau}{\nu/u^2{}_\tau} \tag{5}$$

where ρ_p is the particle density. τ was introduced by Zhang et al. (2001) as a representative time scale of the translational motion. Here, we use τ as a scalar measure on how rapidly a fiber responds to changes in the surrounding flow field. The Stokes number St compares the fiber relaxation time scale τ with a representative time scale ν/u_τ^2 of the large-eddy motion in near-wall turbulence.

RESULTS AND DISCUSSIONS

In present work we considered a fully-developed turbulent channel flow at frictional Reynolds number $Re_\tau = u_\tau h/\nu = 360$. The flow is driven by a constant pressure-gradient. The governing equations (1) are integrated on a three-dimensional domain as well as in time by means of the same Navier-Stokes solver used by Zhao et al. (2012). Periodic boundary conditions are imposed in the two homogeneous directions and no-slip conditions are enforced at the channel walls. The domain size is $6h \times 3h \times h$ in streamwise(x), spanwise(y) and wall-normal (z) directions, respectively. The mesh consists of 192^3 grid points in all three directions. Mesh resolution Δx^+=11.6 and Δy^+=5.3 in streamwise and spanwise directions and Δz^+ is from 0.9 to 2.86 in wall-normal direction. The same mesh is employed in the simulations of both particle-laden and -unladen flow. Time step size $\Delta t^+ = 0.036$. Here, and in the following, the superscript + signifies normalization with the viscous scales.

As shown in Table 1, sixteen fiber sets are studied corresponding to Stokes numbers St=1, 5, 30 and 100 with fiber aspect ratio λ=1, 3, 10, 50. Fibers are treated as pointwise, rigid and collision between fiber and wall is fully elastic with consideration of fiber minor-radius. Initially fibers are distributed randomly in an already fully-developed turbulent channel flow and the statistics is sampled after t^+=5400 over a time-window Δt^+=5400.

The slip velocity is an essential quantity in particle-laden flows to which the force on the particles is directly related. The slip velocity therefore plays an essential role in the transfer of mechanical energy between the fluid phase and the particles (see also Zhao et al. 2012). In this section, the authors presented the results for the mean slip velocities and address the influences of Stokes number St and aspect ratio λ.

First, the profiles of mean slip velocity in streamwise direction are shown in Figure 1(a)-(d). All profiles exhibit a similar trend that varies from negative around the wall region to positive in the channel center. But the magnitudes are substantially dependent on the the Stokes number (notice the different scaling of the ordinate axes in Figure 1), i.e. the fiber with large Stokes number leads to a large slip velocity. The same trend has been observed for the spherical

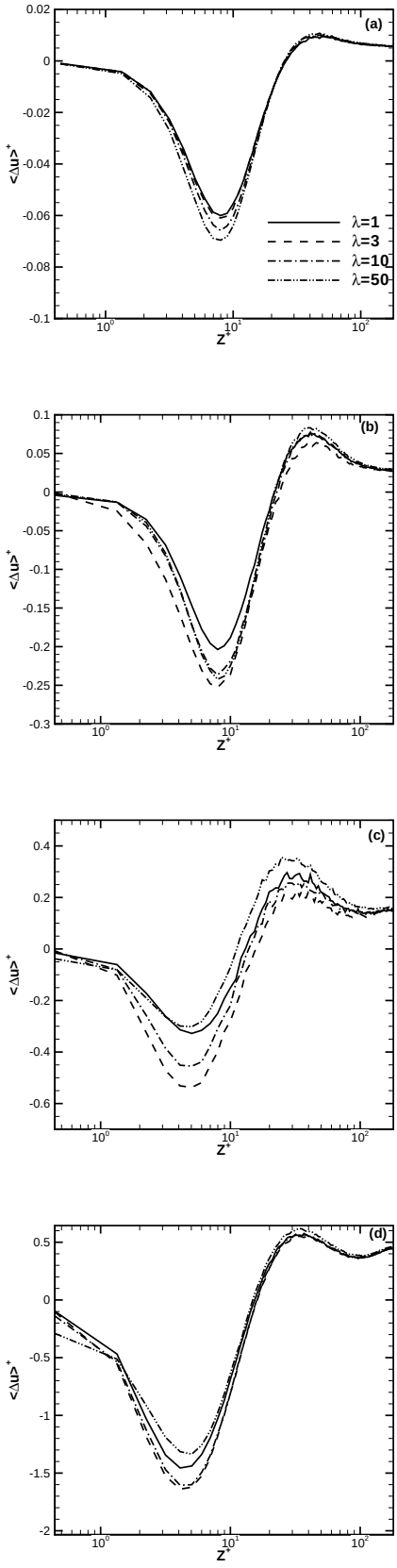

Figure 1. Effect of fiber inertia and elongation on the mean streamwise slip velocity, $\langle \Delta u \rangle^+$. Panels: a) $St = 1$; b) $St = 5$; c) $St = 30$; $St = 100$. Lines: ——— $\lambda = 1$, − − − $\lambda = 3$, − · − · − $\lambda = 10$, − · · − · · − $\lambda = 50$.

Density ratio				
λ \ St	1	5	30	100
1	34.72	173.60	1041.70	3472.33
3	18.57	92.90	557.10	1857.00
10	11.54	57.70	346.30	1154.33
50	7.54	37.69	226.15	753.83

Table 1. 16 sets of fibers with aspect ratio λ=1, 3, 10 and 50 and St=1, 5, 30 and 100. All fibers have the same radius a^+=0.36 on the minor-axis.

particles by Zhao et al. (2012). Additionally center of the negative peak shifts towards the wall with increasing of Stokes number. Secondly, the aspect ratio of the fibers makes the slip velocity variation from the channel wall to the center different from that for spherical particles although the shape of the slip velocity profiles remains the same. The non-monotonic aspect ratio dependence is observed when Stokes number are larger than one, e.g. the case $\lambda = 3$ has minimum value around the negative peak region compared with other cases at $St = 30$ in Figure 1(c).

In Figure 2 the mean slip velocity in wall-normal direction is compared within different Stokes numbers and aspect ratios. Similarly the strong dependence of mean slip velocity on the Stokes number can be also found in wall-normal direction. But a non-linear effect of Stokes number is shown at Stokes number $St = 30$ which has the maximum slip velocity compared with other three Stokes numbers. As we know the hydrodynamic force is proportional to the slip velocity, so the maximum slip velocity in wall-normal direction indicates the most effective deposition of fibers driven by the fluid. A similar conclusion has been also made for the spherical particles(Zhao et al. 2012). The aspect ratio dependence on the mean slip velocity is non-monotonic in wall-normal direction and fibers with $\lambda = 50$ always have minimum value compared with fibers with other aspect ratios. Consequently, the deposition rate of fibers should be lower at $\lambda = 50$ compared with other cases at the same Stokes number.

CONCLUDING REMARKS

In present work the authors performed a one-way coupled DNS of fiber suspensions in a channel flow by using the Euerian-Lagrangian approach. The investigation of mean slip velocity is the main focus. In the statistical results the fibers slip velocities are compared at various Stokes numbers and aspect ratios in the streamwise and wall-normal directions. The effect of Stokes number is found to be important and there is a monotonic dependence that the magnitude of slip velocity becomes larger with increasing Stokes number. However, the influence of aspect ratio is relatively weaker than the Stokes number effect. And a non-monotonic aspect ratio dependence is observed in both streamwise and wall-normal slip velocity. The smallest fiber deposition is found at aspect ratio $\lambda = 50$ with a minimum value of slip velocity in streamwise direction. In general, in the view of mean slip velocity, the fiber behaves similarly as spherical particles in turbulent channel flow.

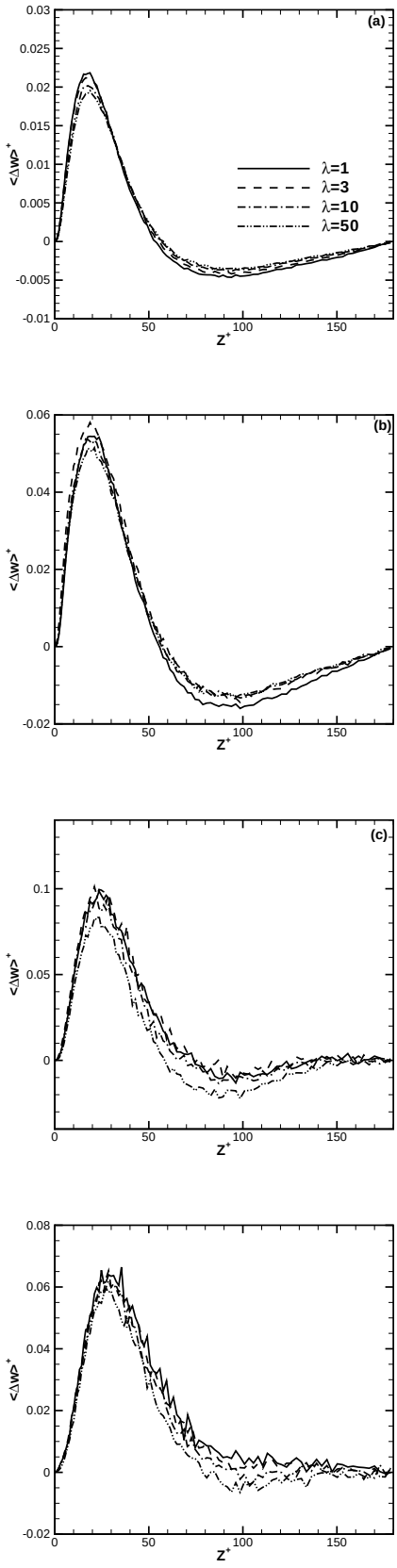

Figure 2. Effect of fiber inertia and elongation on the mean wall-normal slip velocity, $\langle \Delta w \rangle^+$. Panels: a) $St = 1$; b) $St = 5$; c) $St = 30$; $St = 100$. Lines: ——— $\lambda = 1$, – – – $\lambda = 3$, – · – · – $\lambda = 10$, – · · – · · – $\lambda = 50$.

ACKNOWLEDGEMENTS

This study was supported by The Research Council of Norway through project no 213917/F20 "Turbulent particle suspensions". The work has also received support from Research Council of Norway (Programme for Supercomputing) through a grant of computing time. The research work reported herein has benefited from scientific interactions facilitated by COST Action FP1005 funded by European Science Foundation.

REFERENCE

Andersson, H. I., Zhao, L. & Barri, M. 2012 Torque-coupling and particle-turbulence interactions. *Journal of Fluid Mechanics*, **696**, 319-329.

Gillissen,J.J.J.,Boersma, B.J., Mortensen, P.H. & Andersson,H.I. 2008 Fibre-induced drag reduction. *Journal of Fluid Mechanics*, **602**, 209-218.

Lundell, F., & Carlsson, A. 2010 Heavy ellipsoids in creeping shear flow: transitions of the particle rotation rate and orbit shape. *Physical Review E*, **81**, 016323.

Manhart M. 2003 Rheology of suspensions of rigid-rod like particles in turbulent channel flow. *Journal of Non-Newtonian Fluid Mechanics*, **112**, 269-293.

Marchioli, C., Fantoni, M. & Soldati, A. 2010 Orientation, distribution, and deposition of elongated, inertial fibers in turbulent channel flow. *Physics of Fluids*, **22**, 033301.

Mortensen, P.H., Andersson, H.I., Gillissen, J.J.J. & Boersma, B.J. 2008 On the orientation of ellipsoidal particles in a turbulent channel flow. *International Journal of Multiphase Flow*, **34**, 678-683.

Paschkewitz, J.S., Dubief, Y., Dimitropoulos, C.D., Shaqfeh, E.S.G. & Moin P. 2004 Numerical simulation of turbulent drag reduction using rigid fibres *Journal of Fluid Mechanics*, **518**, 281-317.

Zhao, L., Andersson, H.I. & Gillissen, J.J.J. 2012 Interphasial energy transfer and particle dissipation in particle-laden wall turbulence. *Journal of Fluid Mechanics*, **715**, 32-59.